

Adhesion Performance of Steel Bars in Recycled Concrete with Nano-materials in Cold Environments

Yuming ZHANG¹, Xuefeng MEI^{2*}

¹ School of Architecture and Engineering, Weifang University of Science and Technology, Weifang, Shandong, China, 262700

² College of Civil Engineering, Inner Mongolia University of Science and Technology, Baotou, Inner Mongolia, China, 014010

<http://doi.org/10.5755/j02.ms.38941>

Received 26 September 2024; accepted 5 November 2024

This work investigated the adhesion performance of recycled concrete with nano-SiO₂ and nano-Al₂O₃ and steel bars in cold environments through freeze–thaw cycle tests and tensile tests. The results show that the nanomaterials and number of freeze–thaw cycles have no significant effect on the damage morphology of the sample, but the adhesion strength and steel bar slip of the sample are considerably affected by the nanomaterials and number of freeze–thaw cycles. After the addition of the nanomaterials, the adhesion strength increased by 10.4 % (11.2 %), and the steel slip increased, by 17.3 % (16.8 %). The impact of freeze–thaw cycles on adhesion strength and adhesion slip is significant. The adhesion strength decreases by up to 40.8 % after 55 freeze–thaw cycles, and the slip of the steel bar increases by up to 101.9 %. In addition, an adhesion performance model of recycled concrete and steel bars mixed with nanomaterials in cold environments is established. The strengthening mechanism of nanomaterials and the mechanism of freeze–thaw damage is revealed. This study provides a basis for the practical application of recycled concrete technology and promotes the recyclable use of building materials.

Keywords: nano-materials, recycled concrete, rebar, adhesion performance, cold environments.

1. INTRODUCTION

In recent years, the development of recycled concrete (RC) technology has been rapid, but the poor durability of RCs has become a key limiting factor for their application in engineering [1]. Increasing the longevity of RC structures is a significant concern [2]. Techniques for increasing the efficacy of RCs involve aggregate reinforcement and direct reinforcement of concrete [3]. The method of directly strengthening RCs by adding admixtures is more convenient [4].

The incorporation of nanomaterials can fill the gaps in cementitious materials [5] and enhance the bonding at the cement–aggregate interface in concrete [6], thereby increasing the strength and durability of concrete [7]. Nanomineral powders include mainly nano-SiO₂ (NS), nano-Al₂O₃ (NA), and nano-CaCO₃ (NC) [8, 9].

Furthermore, curbing the decline in bond quality between concrete and steel reinforcements in cold climates is crucial for guaranteeing the secure operation of concrete structures [10, 11]. Numerous studies have shown that the adhesion performance between RCs and steel bars deteriorates significantly in cold environments [12, 13]. Many studies have confirmed that the cohesive properties between RCs and steel bars are substantially reduced in frigid environments [14]. In cold climates, the concrete in structures undergoes freeze–thaw damage, which is primarily evident in the persistent growth and permeation of microcracks throughout the internal matrix of the concrete during freeze–thaw action [15, 16]. Adding nanomaterials to concrete can rearrange the internal structure, effectively

preventing the generation of new cracks and the development of existing cracks [17], thereby increasing the density and frost resistance [18]. Additionally, it substantially increases the interfacial adhesion between the concrete and steel bars under freeze–thaw conditions.

Many studies have indicated that nanomaterials can increase the frost resistance of concrete. Bao et al. [19] examined the consequences of assorted NS quantities on the cold resistance of RCs. The results revealed that with increasing NS dosage, the frost resistance of RC continued to improve. Notably, the maximum NS dosage in this experiment was 3 %. Through microstructure analysis, it was discovered that incorporating NS can mitigate the progression of microcracks in concrete and decrease the number of internal pores in RCs. Liu et al. [20] highlighted that the introduction of NS can refine the internal interface zone of concrete and effectively increase its frost resistance. Through analysis, it was discovered that NS can increase the freeze–thaw lifespan of concrete by no less than 43 %. According to Wang et al. [21], the frost resistance of NS-amended concrete in icy regions (temperatures below –20°C) significantly improved, and the performance of the concrete with NS added after 200 freeze–thaw cycles (FTCs) was better than that of the concrete without NS added after 100 FTCs. Behfarnia et al. [22] conducted a study on the impact of NS and NA on the frost durability of concrete and reported that concrete with NA had a more pronounced frost resistance than concrete with NS. Zhang et al. [23] analyzed the response of recycled aggregate concrete to the simultaneous effects of compression and saltwater freezing with the aid of air-entraining agents (AEA) and NS. These

* Corresponding author: X. Mei
E-mail: xfmei@my.swjtu.edu.cn

results indicate that mixing AEA and NS can optimize the salt freezing resistance of RCs. The combined use of AEA and NS can enhance the microstructure of RCs, thereby improving their mechanical and durability properties. Shi et al. [24] analyzed the influence of combining siliconized rubber (SR) with NS on the frost endurance of concrete. The experimental data revealed that the fusion of SR and NS had a cooperative effect, promoting even pore distribution within the concrete and mitigating freeze–thaw damage.

In addition, some scholars have studied the influence of nanomaterials on the adhesion performance of steel bars in concrete. Wang et al. [25] studied the adhesion performance between various nanomaterials and steel bars and reported that the integration of nanomaterials augmented the adhesive interaction between the concrete and steel bars and that the ultimate adhesion strength increased by 10.3 %. Fan et al. [26] reported that NS can increase the interfacial adhesion between RCs and steel bars. The best effect is achieved when the NS dosage is 3 %, which can increase the adhesion strength by 20.52 %. Ismael et al. [27] noted that NS particles and NA particles can increase the adhesion strength of steel bars in concrete, thereby improving the adhesion performance between concrete and steel bars. Musab Alhawwat et al. [28] explored the consequences of NS on the anchorage depth of steel bars in recycled aggregate concrete and assessed the implications of steel bar corrosion on the adhesive interaction between NS-modified RC and steel bars. Yang et al. [29] delved into the consequences of nanomaterials on the adhesive interaction between concrete and steel reinforcements when subjected to chloride-induced deterioration and freeze–thaw action and investigated the underlying improvement mechanism. Research has shown that the integration of NS and nano-TiO₂ (NT) can augment the adhesive interaction between the concrete and steel bars under the coupling of chloride erosion and FTCs, not only increasing the adhesion strength but also reducing the amount of slipping. This occurred because nanoparticles promote the formation of C-S-H gel, reduce the internal porosity of the concrete, and thus improve the adhesion force between the concrete and rebar.

In summary, the addition of nanomaterials can not only improve the frost resistance of concrete but also effectively enhance the adhesion performance between the concrete and steel bars. Therefore, nanomaterials can function as a powerful technique to increase the interfacial adhesion between RCs and steel bars in cold climates, thereby promoting the widespread application of RCs in engineering. However, there is a lack of research on the bond integrity between RCs with nano additives and steel bars. This work studies the effects of the addition of different nanomaterials, different amounts of nanomaterials, and different FTCs on the adhesion performance between RC and steel bars and

establishes a calculation model for the strength and slip between RC and steel bars with nanomaterials in cold climates, providing a theoretical basis for the application of RCs with nanomaterials in cold region engineering.

2. TEST METHOD

2.1. Materials

The three-day compressive strength and three-day flexural strength of the PO 42.5 cement used in this experiment are 27.8 MPa and 5.3 MPa, respectively, whereas the twenty-eight-day compressive strength and three-day flexural strength are 47.8 MPa and 9.2 MPa, respectively, which meet the relevant requirements of GB 175-2007 [30]. The fine aggregate comprises manufactured sand with a grading modulus of 2.8. The specific performance indicators of recycled coarse aggregate obtained by crushing and screening waste concrete are shown in Table 1 and meet the relevant requirements of GB/T 14685-2022 [31]. NS and NA were chosen as nanomaterials and were characterized by a particle diameter of 20 nm and specific surface areas of 230 m²/g and 110 m²/g (according to the Brunauer-Emmett-Teller (BET) testing method), respectively.

Table 1. Properties of the coarse aggregates

Type	Size, mm	Water absorption, %	Crushing index, %
RA*	4.75–22.5	9.8	15.9
FA*	2.3–3.0	4.5	–

RA* represents the recycled coarse aggregate, and FA* represents the fine aggregate.

The steel bars utilized in the pull-out samples included HRB400 deformed steel bars as stressed steel bars and HPB300 round steel bars as stirrups. The particular performance measures of the steel bars are detailed in Table 2.

Table 2. Properties of the steel bar

Type		Diameter, mm	Yield strength, MPa
Stressed steel bar	HRB400	20	520
Stirrup	HPB300	8	398

2.2. Concrete mix design

The mix ratio of RCs is designed according to JGJ 55-2019 [32]. The target strength of RC is 35 MPa, and the dosages of NS and NA are 1 %, 2 %, and 3 % (replace cement with equivalent quality), respectively, as shown in Table 3.

Table 3. Concrete mixture, kg/m³

Type	Cement	Water	Fine aggregate	RA	NS	NA
RC	395	195	598	1085	0	0
RC-NS-1	391	195	598	1085	4.0	0
RC-NS-2	387.1	195	598	1085	7.9	0
RC-NS-3	383.1	195	598	1085	11.9	0
RC-NA-1	391	195	598	1085	0	4.0
RC-NA-2	387.1	195	598	1085	0	7.9
RC-NA-3	383.1	195	598	1085	0	11.9

2.3. Specimen design

With a cross-sectional measurement of 100 mm × 100 mm, the pull-out sample is 180 mm in length, as shown in Fig. 1. The anchorage length of the concrete and steel bars is 150 mm, with other areas being segmented by a PVC pipe to avoid stress concentration at the loading zone.

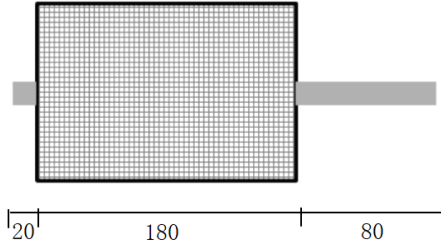


Fig. 1. Pullout specimen size

2.3. Freeze-thaw damage test

In this study, a hydraulic servo testing machine was used to test the adhesion performance, and a load sensor and displacement sensor were used to test the adhesion strength and adhesion slip value simultaneously [33], as shown in Fig. 2. After the curing phase (28 days in total), the samples were sunk in the sample case and placed in a rapid freeze-thaw cycle machine, as demonstrated in Fig. 2.

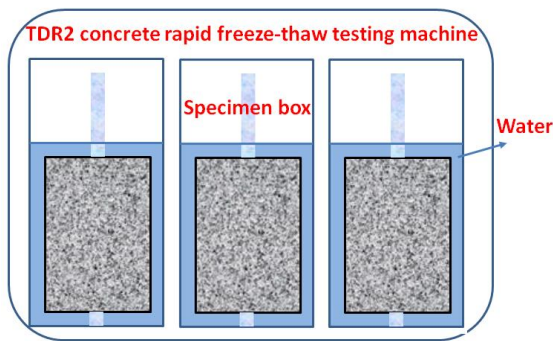


Fig. 2. Freeze-thaw damage test

The frost-thaw degradation examination was performed in accordance with the designated criteria of GB/T 50082-2009 [33]. The groupings of the freeze-thaw cycle (FTC) samples are detailed in Table 4, and the maximum number of freeze-thaw cycles is 55.

Table 4. Grouping of FTC samples

Type	Number of FTCs
RC-NS-3	0, 10, 25, 35, 45, 55
RC-NA-3	0, 10, 25, 35, 45, 55

2.4. Adhesion performance test

The adhesion performance of the samples that completed the freeze-thaw cycle test was tested. In this study, a hydraulic servo testing machine was used to test the adhesion performance to JGJT 152-2019 [34], the displacement loading rate was 0.4 mm/min, and a load sensor and displacement sensor were used to test the adhesion strength and adhesion slip value simultaneously [35], as shown in Fig. 3.

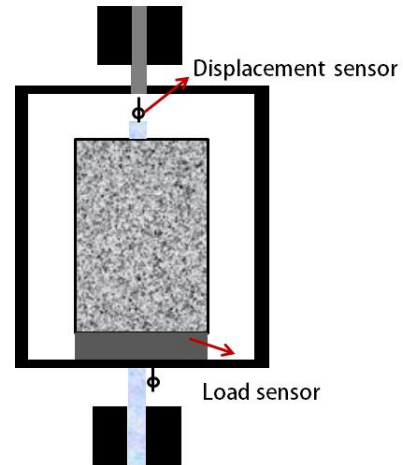


Fig. 3. Load diagram of adhesion performance

3. RESULTS AND ANALYSIS

3.1 Damage morphology

The damage morphologies of each group of samples are similar. During the loading process, cracks begin to appear near the loading end of the concrete samples, and the cracks continue to develop with increasing load. When the loading is complete, the main crack running through the whole sample appears, but the sample is still not a whole, which conforms to the form of pull-out splitting damage [14], as shown in Figure 4. Following the incorporation of nanomaterials and FTCs, there was no substantial alteration in the damage morphology of the sample, suggesting that the nanomaterials and FTCs did not modify the primary damage progression of the sample.



Fig. 4. Adhesion damage morphology

3.2. Influence of NSs and NAs on adhesion performance

The influences of NS and NA on adhesion performance are shown in Fig. 5, Fig. 6, and Fig. 7, respectively. The adhesion strength of the RC pull-out samples was 13.8 MPa, which was lower than that of ordinary concrete pull-out samples with the same mix proportion [12]. The main reasons are as follows: on the one hand, recycled aggregates cause initial damage during the crushing process, resulting in poor aggregate performance, which in turn affects the strength of concrete samples [13]; on the other hand, the presence of three weak zones (i.e., interface transition zones) within RCs is bound to affect the strength of concrete samples [14]. After adding NS and NA, the adhesion strength of the steel bars in the concrete improved, whereas the slip value of the steel bars decreased, which means that

the adhesion performance of the steel bars in the RC improved. Cui [5] reported that the dosage of nanomaterials could enhance the mechanical properties of concrete, which was also the key to improving its adhesion performance with steel bars.

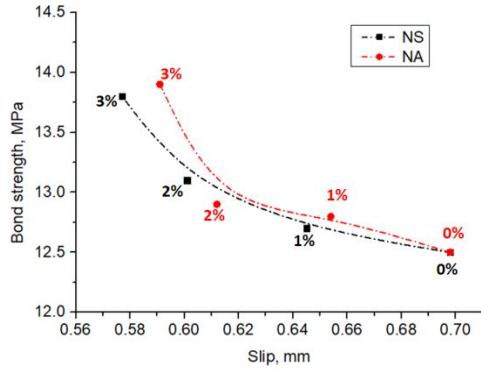


Fig. 5. Relationship between the adhesion strength and slip

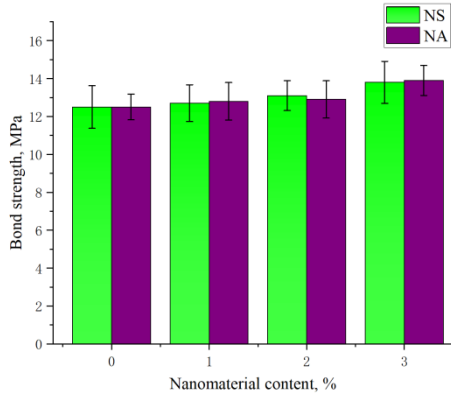


Fig. 6. Influence of NS and NA on the adhesion strength

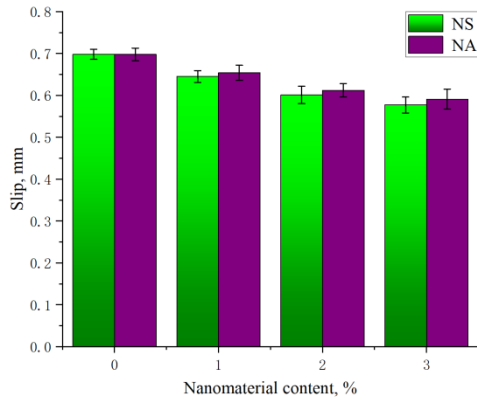


Fig. 7. Influence of NS and NA on steel bar slip

NS resulted in a minimum increase of 1.6 % in adhesion strength, whereas NA resulted in a minimum increase of 2.4 % in adhesion strength. The NS minimum reduced the slip of the steel bars by 7.6 %, whereas the NA minimum reduced the slip of the steel bars by 6.3 %. When the dosage of NS (NA) was 3 %, the improvement effect of the nanomaterials on the adhesion performance of the steel bars in the concrete was optimal, with a 10.4 % (11.2 %) increase in the adhesion performance and a 17.3 % (16.8 %) decrease in the steel bar slip value. This is attributed to the pozzolanic reaction of NS, which has a supplementary hydration interaction with $\text{Ca}(\text{OH})_2$. With increasing time, NS

interacts with $\text{Ca}(\text{OH})_2$ from cement hydration to undergo further hydration, resulting in the creation of C-S-H gel, which increases the density of the concrete. NA engages with C-S-H gel, a product of hydration, to create C-A-H or C-A-S-H, thus increasing the density of the concrete and improving the strength of the RC itself, increasing the friction and mechanical biting force between it and the steel bar and improving the adhesion performance [36].

3.3. Adhesion performance model of RC and steel bars mixed with nanomaterials

The relationships between the content of the nanomaterials and the adhesion strength and between the content of the nanomaterials and the slip were obtained through data analysis, as shown in Fig. 8 and Fig. 9.

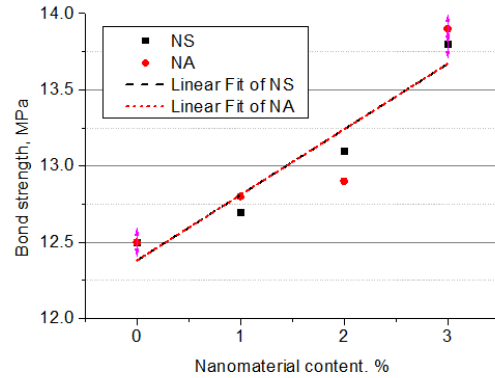


Fig. 8. Relationship between the nanomaterial content and adhesion strength

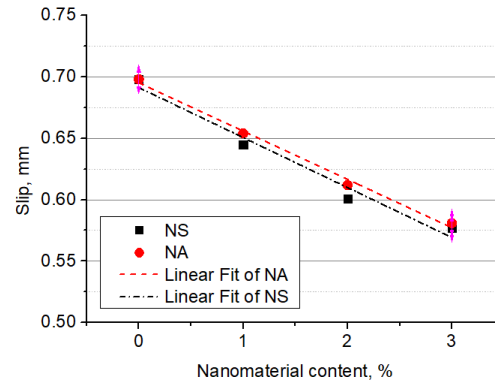


Fig. 9. Relationship between the nanomaterial content and steel bar slip

The fitting model for the adhesion strength is consistent, indicating that the effects of different nanomaterials on the cohesive strength are trivial (B is the adhesion strength, S is the steel bar slip, and x is the nanomaterial content).

Adhesion strength of NS:

$$B = 0.43x + 12.38 \quad R^2 = 0.9362. \quad (1)$$

Adhesion strength of NA:

$$B = 0.43x + 12.38 \quad R^2 = 0.8348. \quad (2)$$

Steel bar slip of the NS:

$$S = -0.0407x + 0.6913 \quad R^2 = 0.9745. \quad (3)$$

Steel bar slip of NA:

$$S = -0.0393x + 0.6953 \quad R^2 = 0.9940. \quad (4)$$

3.4. Influence of freeze-thaw damage on adhesion performance

The influence of freeze-thaw damage on adhesion performance is shown in Fig. 10, Fig. 11, and Fig. 12, respectively. The influence of FTCs on the two key indicators of adhesion performance is quite significant, and the adhesion strength tends to decrease [37], especially after 35 cycles, and the adhesion strength significantly decreases.

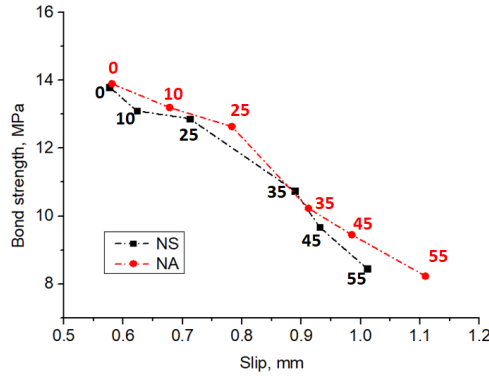


Fig. 10. Relationship between adhesion strength and slip after FTCs

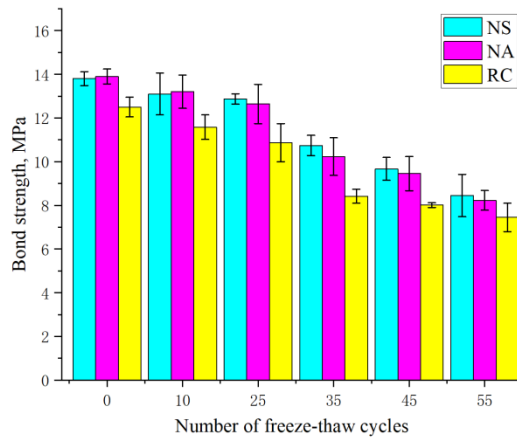


Fig. 11. Influence of freeze-thaw damage on the adhesion strength

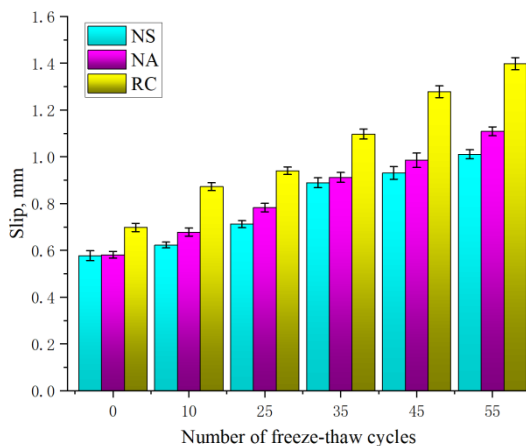


Fig. 12. Influence of freeze-thaw damage on steel bar slip

During this period, the RC samples blended with NS experienced a 22.2 % reduction in adhesion strength, whereas the recycled concrete samples with NA experienced a 26.4 % decrease in adhesion strength. Moreover, the steel slip value also significantly increased, and the steel slip

growth rate of the recycled concrete samples mixed with NS was 88.9 %; the slip growth rate of the steel bars in the recycled concrete samples mixed with NA was 91.2 %. Upon reaching the maximum FTC, the recycled concrete samples blended with NS exhibit a 38.7 % reduction in adhesion strength, whereas those mixed with NA show a 40.8 % decrease. For the RC samples mixed with NS, the growth rate of the steel bar slip was 101.1 %, whereas for those mixed with NA, it was 101.9 %. The change in steel slip after the FTCs is very significant. This is because freeze-thaw cycles cause damage to the recycled concrete sample from the outside to the inside, and cracks continue to propagate inward from the outside of the sample. Upon the crack breaching the adhesion interface between the steel bar and the concrete, there is a marked reduction in the concrete's capacity to restrain the steel bar, leading to a substantial increase in the steel slip value [38].

The adhesion performance of RCs without nanomaterials decreased more significantly. After 55 FTCs, the adhesion strength decreased by 40.4 %, and the bond slip increased by 114.2 %. The nanomaterials improved the frost resistance of the RC and steel bar samples. Gong [6] noted that nanomaterials could effectively improve the frost resistance of RCs, which was also the reason for the improved adhesion performance between RCs and steel bars in freeze-thaw environments after the addition of nanomaterials. In addition, with a further increase in the number of FTCs, the advantages of adding nanomaterials to recycled concrete samples become more significant. Furthermore, in cold environments, the difference in adhesion performance between RC samples with the addition of two types of nanomaterials is not significant. The maximum difference in the adhesion strength change rate amidst a consistent freeze-thaw climate is 4.2 %, and the maximum difference in the steel slip change rate is 9.8 %.

3.5. Adhesion performance model of recycled concrete and steel bars mixed with nanomaterials in cold environments

The relationships between the number of FTCs and the adhesion strength and the relationship between the content of nanomaterials and the slip of the steel bars are obtained through data analysis, as shown in Fig. 13 and Fig. 14 ($B(n)$ is the adhesion strength in cold environments, $S(n)$ is the steel bar slip in cold environments, and n is the number of freeze-thaw cycles).

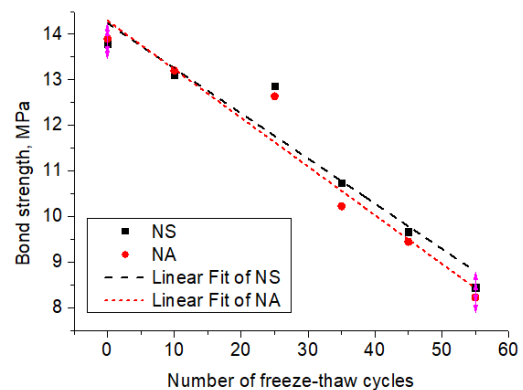


Fig. 13. Relationship between the number of FTCs and the adhesion strength

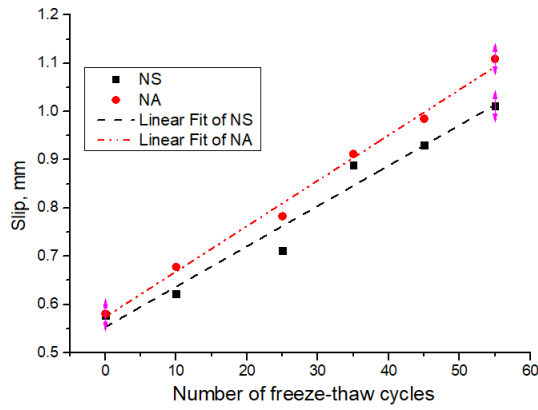


Fig. 14. Relationship between the number of FTCs and the degree of steel bar slip

Adhesion strength of NS:

$$B(n) = -0.0978n + 14.094 \quad R^2 = 0.9797. \quad (5)$$

Adhesion strength of NA:

$$B(n) = -0.1058n + 14.183 \quad R^2 = 0.9806. \quad (6)$$

Steel bar slip of the NS:

$$S(n) = 0.0084n + 0.5535 \quad R^2 = 0.9674. \quad (7)$$

Steel bar slip of NA:

$$S(n) = 0.0094n + 0.5744 \quad R^2 = 0.9930. \quad (8)$$

3.6. Mechanistic analysis

3.6.1. Strengthening mechanism of nanomaterials

The improvement in the adhesion performance of recycled concrete samples by nanomaterials is reflected mainly in their enhancement of the properties of the recycled concrete materials themselves, and their effects are reflected mainly in the following aspects [39]:

1. Pore-filling impact of nanomaterials. Their tiny particle size and substantial specific surface area allow them to occupy the micropores in the concrete, lower the porosity, and thereby increase the solidity and strength of the concrete.
2. Volcanic ash effects of nanomaterials. Nanomaterials can react with cement hydration products to form more C-S-H gel, thus improving the performance of concrete [5, 6].
3. The surface activity of nanomaterials. The high surface energy of nanomaterials can promote the hydration reaction of cement, accelerate the hardening process of cement slurries, and improve the early strength of concrete.
4. The nucleation effect of nanomaterials. Nanomaterials can serve as crystal nuclei for hydration products, promoting their generation and growth, which leads to better mechanical characteristics of the concrete.
5. Improving the interface transition zone via nanomaterials. Nanomaterials can improve the ITZ between recycled aggregates and cement slurry, enhancing the overall performance of concrete.
6. Nanopore structure characteristics: nanofillers can refine nanointerlayers and gel pores, causing part of the C-S-H structure to shrink and become dense and

improving the performance of concrete [7].

3.6.2. Mechanism of freeze-thaw damage

The primary sources of deterioration in recycled concrete throughout FTCs are as follows [13]:

1. Internal structural damage: Without the FTC, the water within the concrete solidifies and swells, leading to harm to the internal pore structure and the spread of microcracks, thus diminishing the performance of recycled concrete [15].
2. Deterioration of the ITZ: The interface transition zone between aggregates in recycled concrete and new cement slurry is prone to damage during FTCs due to its porosity and high permeability, resulting in a decrease in adhesion strength.
3. Water absorption and pore structure changes: Freeze thaw cycles can increase the water absorption of concrete, cause changes in the pore structure, and thus affect the performance of recycled concrete [16].

The adhesion force between recycled concrete and reinforcement mainly includes [40]:

1. The chemical adhesion force, which is the chemical adhesion or adsorption force generated by the cement gel in the concrete on the surface of the reinforcement.
2. The friction force, which is the force generated by tightly gripping steel bars after concrete shrinkage. Frictional forces arise at the interface between the steel bars and the concrete when there is relative movement between them.
3. Mechanical bite force: This force is created by the mechanical interaction between the uneven surface of the steel bar and the concrete. The transverse ribs of deformed steel bars generate a mechanical biting force, which is often significant and the main source of adhesion force for deformed steel bars. Among them, the chemical adhesion force is relatively small, whereas the frictional force and mechanical biting force play a more important role in deformed steel bars. Throughout the freeze-thaw cycle, the cracks within the concrete experience damage starting from the exterior and progressing inward until they reach the adhesion surface between the steel bars and the concrete, causing damage to the adhesion surface, as shown in Fig. 15.

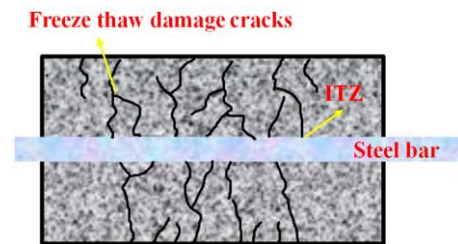


Fig. 15. Schematic diagram of concrete crack development in a freeze-thaw environment

During this process, the first step is the loss of chemical adhesion force, resulting in a lack of restraint force between the concrete and the steel bars in the initial stage of adhesion and loading; subsequently, it leads to the loss of friction and mechanical biting force, causing a rapid decrease in the restraining ability of RC on steel bars, resulting in the degradation of adhesion performance [15].

4. CONCLUSIONS

1. The damage morphology of each group of samples was similar, showing a tensile splitting damage morphology; the nanomaterials and FTCs did not significantly affect the damage morphology of the samples.
2. After adding NS and NA, the adhesion strength between the concrete and steel bars improved, whereas the slip value of the steel bars decreased, the adhesion strength increased by 10.4 % (11.2 %), and the steel slip increased by 17.3 % (16.8 %), which means that the adhesion performance between the RC and steel bars improved.
3. The impact of FTCs on two key indicators of adhesion performance was quite significant, with a decreasing trend in adhesion strength and a significant increase in steel slip value. Upon reaching the maximum FTC, the adhesion strength increases by 38.7 % (40.8 %), and the steel slip increases by 101.1 % (101.9 %).
4. The adhesion performance of the RC sample without nanomaterials decreased more significantly. After 55 FTCs, the adhesion strength decreased by 40.4 %, and the bond slip increased by 114.2 %. Therefore, the nanomaterials improved the frost resistance of the RC samples.
5. An adhesion performance model of RCs and steel bars mixed with nanomaterials in cold environments was established. In addition, the strengthening mechanism of the nanomaterials and the mechanism of freeze-thaw damage were revealed.

Acknowledgments

This work was supported by the Shandong Province Natural Science Foundation Youth Branch (ZR2021QE209).

REFERENCES

1. Awchat, G., Dhanjode, G. Strength and Durability of Recycled Concrete Strengthened with Steel Fibers and Styrene Butadiene Rubber Latex *Advanced Engineering Forum* 44 2023: pp. 1–16. <https://doi.org/10.1016/j.conbuildmat.2022.126967>
2. Xiong, X., Lu, H. Optimisation Method for Durability of Recycled Concrete Based on Nano Strengthening Technology *International Journal of Microstructure and Materials Properties* 17 (1) 2024: pp. 1–16. <https://doi.org/10.1504/IJMMP.2024.135797>
3. Zhou, Y., Zhuang, J., Xu, W., Lin, W., Xing, F., Hu, R. Study on Mechanical Performance and Mesoscopic Simulation of Nano-SiO₂ Modified Recycled Aggregate Concrete *Construction and Building Materials* 425 2024: pp. 136053. <https://doi.org/10.1016/j.conbuildmat.2024.136053>
4. Wang, T., Wang, Q.S., Cui, S.A., Yi, H.H., Su, T., Tan, Z. Effects of Nano-materials Reinforced Aggregate on Mechanical Properties and Microstructure of Recycled Brick Aggregate Concrete *Materials Science (Medžiagotyra)* 29 (3) 2023: pp. 347–355. <https://doi.org/10.5755/j02.ms.32715>
5. Cui, S.A., Wang, T., Gong, S.W., Ren, X.Y., Li, M., Su, T., Tan, Z.Y., Cao, F.B., Li, B.X. Strengthening Effect of Nano-materials on the Compressive Strength and Microstructure of Recycled Brick Aggregate Concrete *Materials Science (Medžiagotyra)* 30 (2) 2024: pp. 239–247. <https://doi.org/10.5755/j02.ms.35298>
6. Gong, S.W., Wang, T., Hasan, H.H., Mei, X.F., Tan, Z.Y., Su, T., Cao, F.B. Effect of Polypropylene Fiber and Nanosilica on the Compressive Strength and Frost Resistance of Recycled Brick Aggregate Concrete *Nanotechnology Reviews* 12 (1) 2023: pp. 20230174. <https://doi.org/10.1515/ntrev-2023-0174>
7. Su, T., Wang, T., Zhang, Z.C., Sun, X., Gong, S.W., Mei, X.F., Cui, S.A., Tan, Z.Y. Mechanical Properties and Frost Resistance of Recycled Brick Aggregate Concrete Modified by Nano-SiO₂ *Nanotechnology Reviews* 12 (1) 2023: pp. 20230576. <https://doi.org/10.1515/ntrev-2023-0576>
8. Wang, D., Liu, K., Kang, M., Han, L. Experimental Study on the Bond Performance Between Ultra-high Performance Concrete and Steel Bar under Freeze-thaw Cycles *Case Studies in Construction Materials* 20 2024: pp. 03401. <https://doi.org/10.1016/j.cscm.2024.e03401>
9. Sun, H., Luo, L., Yuan, H., Li, X. Experimental Evaluation of Mechanical Properties and Microstructure for Recycled Aggregate Concrete Collaboratively Modified with Nanosilica and Mixed Fibers *Construction and Building Materials* 403 2023: pp. 133125. <https://doi.org/10.1016/j.conbuildmat.2023.133125>
10. Shah, I., Li, J., Khan, N.R., Almujaib, H., Rehman, M., Raza, A., Peng, Y. Bond-Slip Behavior of Steel Bar and Recycled Steel Fibre-Reinforced Concrete *Journal of Renewable Materials* 12 (1) 2024: pp. 167–186. <https://doi.org/10.32604/jrm.2023.031503>
11. Liu, K.H., Yan, J.C., Meng, X.X., Zou, C.Y. Bond Behavior Between Deformed Steel Bars and Recycled Aggregate Concrete after Freeze-thaw Cycles *Construction and Building Materials* 232 2020: pp. 117236. <https://doi.org/10.1016/j.conbuildmat.2019.117236>
12. Shang, H.S., Zhao, T.J., Cao, W.Q. Bond Behavior Between Steel Bar and Recycled Aggregate Concrete after Freeze-thaw Cycles *Cold Regions Science and Technology* 118 2015: pp. 38–44. <https://doi.org/10.1016/j.coldregions.2015.06.008>
13. Su, T., Wang, T., Wang, C.G., Yi, H.H. The Influence of Salt-frost Cycles on the Bond Behavior Distribution Between Rebar and Recycled Coarse Aggregate Concrete *Journal of Building Engineering* 45 2022: pp. 103568. <https://doi.org/10.1016/j.job.2021.103568>
14. Su, T., Wang, C.X., Cao, F.B., Zou, Z.H., Wang, C.G., Wang, J., Yi, H.H. An Overview of Bond Behavior of Recycled Coarse Aggregate Concrete with Steel Bar *Reviews on Advanced Materials Science* 60 (1) 2021: pp. 127–144. <https://doi.org/10.1515/rams-2021-0018>
15. Su, T., Huang, Z.F., Yuan, J.F., Zou, Z.H., Wang, C.G., Yi, H.H. Bond Properties of Deformed Rebar in Frost-damaged Recycled Coarse Aggregate Concrete under Repeated Loadings *Journal of Materials in Civil Engineering* 34 (10) 2022: pp. 04022257. [https://doi.org/10.1061/\(ASCE\)MT.1943-5533.0004401](https://doi.org/10.1061/(ASCE)MT.1943-5533.0004401)
16. Wang, T., Yang, X.C., Yang, D.Q., Mei, X.F., Su, T. Bond Performance of Recycled Coarse Aggregate Concrete with Rebar under Freeze-thaw Environment: A review *Nonlinear Engineering* 13 (1) 2024: pp. 20240001. <https://doi.org/10.1515/nleng-2024-0001>

17. Ashwini, K., Rao, P.S. Freeze and Thaw Resistance of Concrete using Alccofine and Nano-silica *Materials Today: Proceedings* 47 2021: pp. 4336–4340.
<https://doi.org/10.1016/j.matpr.2021.04.629>
18. Liu, J., Xu, S., Li, L., Zhang, G. Freeze-thaw Cycling of Nano-SiO₂-modified Recycled Aggregate in Concretes: hydro-thermal-mechanical modeling *Journal of Building Engineering* 96 2021: pp. 110554.
<https://doi.org/10.1016/j.jobbe.2024.110554>
19. Bao, J., Zhang, H., Ding, Y., Chen, X., Zhang, P., Xue, S., Qin, L., Song, Q. Salt-frost Scaling Resistance Characteristics of Nano Silica-modified Recycled Aggregate Concrete *Journal of Building Engineering* 91 2024: pp. 109674.
<https://doi.org/10.1016/j.jobbe.2024.109674>
20. Liu, F., Tang, R., Ma, W., Yuan, X. Analysis on Frost Resistance and Pore Structure of Phase Change Concrete Modified by Nano-SiO₂ under Freeze-thaw Cycles *Measurement* 230 2024: pp. 114524.
<https://doi.org/10.1016/j.measurement.2024.114524>
21. Wang, C., Zhang, M., Pei, W., Lai, Y., Dai, J., Xue, Y., Sun, J. Frost Resistance of Concrete Mixed with Nano-silica in Severely Cold Regions *Cold Regions Science and Technology* 217 2024: pp. 104038.
<https://doi.org/10.1016/j.coldregions.2023.104038>
22. Behfarnia, K., Salemi, N. The Effects of Nano-silica and Nano-alumina on Frost Resistance of Normal Concrete *Construction and Building Materials* 48 2013: pp. 580–584.
<https://doi.org/10.1016/j.conbuildmat.2013.07.088>
23. Zhang, H., Luo, G., Bao, J., Zhang, P., Lv, H., Li, Y., Song, Q. Improving the Salt Frost Resistance of Recycled Aggregate Concrete Modified by Air-entraining Agents and Nano-silica under Sustained Compressive loading *Case Studies in Construction Materials* 20 2024: pp. e03170.
<https://doi.org/10.1016/j.cscm.2024.e03170>
24. Shi, J., Zhao, L., Han, C., Han, H. The Effects of Silanized Rubber and Nano-SiO₂ on Microstructure and Frost Resistance Characteristics of Concrete Using Response Surface Methodology (RSM) *Construction and Building Materials* 344 2022: pp. 128226.
<https://doi.org/10.1016/j.conbuildmat.2022.128226>
25. Wang, X., Dong, S., Ashour, A., Ding, S., Han, B. Bond Behaviors Between Nano-engineered Concrete and Steel Bars *Construction and Building Materials* 299 2021: pp. 124261.
<https://doi.org/10.1016/j.conbuildmat.2021.124261>
26. Fan, C.C., Zheng, Y.X., Zhuo, J.B., Du, C.W., Hu, S.W. Study on Mechanical and Bonding Properties of Nano-SiO₂ Reinforced Recycled Concrete: Macro Test and Micro Analysis *Journal of Building Engineering* 94 2024: pp. 109877.
<https://doi.org/10.1016/j.jobbe.2024.109877>
27. Ismael, R., Silva, J.V., Carmo, R.N.F., Soldado, E., Lourenço, C., Costa, H., Júlio, E. Influence of Nano-SiO₂ and Nano-Al₂O₃ Additions on Steel-to-concrete Bonding *Construction and Building Materials* 125 2016: pp. 1080–1092.
<https://doi.org/10.1016/j.conbuildmat.2016.08.152>
28. Alhawati, M., Ashour, A. Bond Strength Between Corroded Steel and Recycled Aggregate Concrete Incorporating Nano Silica *Construction and Building Materials* 237 2020: pp. 117441.
<https://doi.org/10.1016/j.conbuildmat.2019.117441>
29. Yang, H., Liu, K., Zhang, M., Sun, S., Li, T. Bond Performance of Marine Concrete with Nano-particles to Steel Bars under the Action of Both Cl-erosion and Freeze-thaw Cycles *Journal of Building Engineering* 95 2024: pp. 110105.
<https://doi.org/10.1016/j.jobbe.2024.110105>
30. GB 175-2007. Common Portland Cement. China Standardization Administration, Beijing, 2007. (in Chinese)
31. GB/T 14685-2022. Pebble and Crushed Stone for Construction. Beijing: State market regulatory administration, Beijing, 2022. (in Chinese)
32. JGJ 55-2019. Specification for Mix Proportion Design of Ordinary Concrete. Beijing: China Architecture and Building Press, Beijing, 2019. (in Chinese)
33. GB/T 50082-2009. Standard for Test Method of Long-Term Performance and Durability of Ordinary Concrete. China Academy of Building Research, China, 2009. (in Chinese)
34. JGJT 152-2019. Technical Specification for Steel Reinforcement Testing in Concrete. Ministry of Housing and Urban-Rural Development of the People's Republic of China, China, 2009. (in Chinese)
35. GB/T 50081-2019. Standard for Test Methods of Concrete Physical and Mechanical Properties, China Academy of Building Research, China, 2019. (in Chinese)
36. Su, T., Wu, J., Zou, Z.H., Yuan, J.F. Bond Performance of Steel Bar in RAC under Salt-frost and Repeated Loading *Journal of Materials in Civil Engineering* 32 (9) 2020: pp. 04020261.
<https://doi.org/10.1016/j.conbuildmat.2019.07.301>
37. Ren, G.S., Shang, H.S., Zhang, P., Zhao, T.J. Bond Behaviour of Reinforced Recycled Concrete after Rapid Freezing-thawing Cycles *Cold Regions Science and Technology* 157 2019: pp. 133–138.
<https://doi.org/10.1016/j.coldregions.2018.10.005>
38. Li, Z.H., Deng, Z.H., Yang, H.F., Wang, H.L. Bond Behavior Between Recycled Aggregate Concrete and Deformed Rebar after Freeze-thaw Damage *Construction and Building Materials* 250 2020: pp. 118805.1–11.
<https://doi.org/10.1016/j.conbuildmat.2020.118805>
39. Huang, C., Nantung, T., Feng, Y., Lu, N. Effect of Colloidal Nano Silica on the Freeze-thaw Resistance and Air Void System of Portland Cement Concrete *Journal of Building Engineering* 86 2024: pp. 108888.
<https://doi.org/10.1016/j.jobbe.2024.108888>
40. Kim, S.W., Yun, H.D., Park, W.S., Jang, Y.I. Bond Strength Prediction for Deformed Steel Rebar Embedded in Recycled Coarse Aggregate Concrete *Materials and Design* 83 (10) 2015: pp. 257–269.
<https://doi.org/10.1016/j.matdes.2015.06.008>

